# Supporting Information

Zhang *et al.* 10.1073/pnas.0801349105

## SI Text

**X-Ray Diffraction Analysis of ZnPc-SWNHox-BSA.** X-ray diffraction (XRD) analysis of dried ZnPc-SWNHox, ZnPc, and ZnPc-SWNHox-BSA. XRD was measured with a Cu line (k$\alpha$, k$\beta$: $\lambda$ = 1.54, 1.39 Å) generated at 45 kV and 40 mA. There was no peak originating from the ZnPc crystals in either ZnPc-SWNHox and ZnPc-SWNHox-BSA (Fig. S1), in agreement with the observations by TEM that most of ZnPc molecules were loaded on SWNHox.

**Dispersion of ZnPc-SWNHox-BSA.** Freeze-dried ZnPc-SWNHox-BSA was dispersed in PBS (0.1 mg/ml) by sonication for 3 min in a bath-type sonicator. The obtained dispersion was stable for several weeks (Fig. S2 *Inset*) at least. The dispersion was measured with a dynamic light scattering method, using a laser with a wavelength of 633 nm (FPAR-1000; Photal Otsuka Electronics). Fig. S2 shows that the major particles of ZnPc-SWNHox-BSA were ≈160 nm in size.

**The Body Weight of Mice in the Testing Period of PDT-PHT.** Fig. S3 shows changes in body weight of mice during the PDT-PHT testing period. Injection of ZnPc, SWNHox-BSA, ZnPc-SWNHox-BSA, or PBS did not cause weight loss.

**Discussion on Mechanism of the PDT by Using ZnPc-SWNHox-BSA.** ***Detection of singlet oxygen.*** ADPA (0.37 mg; anthracene-9,10-dipropionic acid disodium salt; Molecular Probes) was dissolved in 100 ml of PBS (ADPA, 10 $\mu$M) and mixed with the ZnPc-SWNHox-BSA dispersion in PBS (ZnPc, 10 $\mu$M) with a volume ratio of 1:1. The resulting mixture (4 ml) was irradiated with 650–750 nm light (Xe lamp, filtered by band-path filter, 100 mW) for 0–10 min. The absorption spectra of ADPA dissolved in the dispersion of ZnPc-SWNHox-BSA in PBS were measured by UV-Vis-NIR spectrometer (Lambda 19; PerkinElmer) and showed that the absorption band of ADPA, for example, at 358, 378, and 400 nm did not change after light irradiation. This indicated that no singlet oxygen was generated.

***Photoinduced charge-transfer in the ZnPc-SWNHox-BSA system and potential reactive oxygen generation.*** Optical absorption spectra of the aqueous solution of ZnPc-SWNHox-BSA showed absorption bands at 602 and 666 nm, which are characteristic of ZnPc. These absorption bands red-shifted to 635 and 710 nm, respectively, and the bandwidth broadened compared with those of ZnPc dissolved in ethanol (Fig. S4*b*). These data indicate that ZnPc interacted strongly with SWNHox.

The spectra in Fig. S4*c* suggest that photoinduced charge separation between ZnPc and SWNHox generates an electron hole and an electron as the first step, then the electron is extracted by $MV^{2+}$ to generate $MV^{\bullet+}$. Meanwhile, BNAH donates an electron to $ZnPc^{\bullet+}$, retarding the consumption of $MV^{\bullet+}$ by back electron transfer to $ZnPc^{\bullet+}$. These processes are illustrated in Fig. S5.

When oxygen is present, it can accept electrons from the charge separated state of ZnPc-SWNHox-BSA to generate $O_2^{\bullet-}$. The possible processes are shown in Fig. S6.

**Photothermal Effect.** To confirm the photothermal effect, we monitored the temperature of PBS solutions of dispersed ZnPc-SWNHox-BSA and SWNHox-BSA during 670-nm laser irradiation (Fig. S7).

**Agar Tissue-Mimicking Phantom Experiment.** We performed an agar tissue-mimicking phantom experiment to investigate whether PHT increased tissue temperature (Fig. S8). The agar gel consisted of 2.0% agar and 0.5% NaCl (% by weight) (1), and SWNHox-BSA or ZnPc-SWNHox-BSA (SWNHox, 0, 0.01, or 0.001% by weight). We made the gel as corded structures (2) with diameter of ≈1 mm and length of ≈3–5 mm and loaded them into a 10-ml syringe to construct a cylindrical phantom. Saline solution (0.35%), which has an electrical conductivity close to that of blood (3), was pumped into a small reservoir at the top of the phantom. The flow rate was about 1.25 ml/min ($\approx 2.4 \times 10^{-6}$ $m^3/s/kg$ phantom). This provided a cooling effect similar to that provided by flowing blood in muscle tissue according to the calculation (2). The phantom was irradiated for 0–10 min by using the same 670-nm laser used in the mouse experiments, and the temperature of the phantom was measured by using a chromel-alumel thermocouple thermometer inserted into phantom, ≈3 mm close to the wall of syringe (Fig. S8).

The temperature in the phantoms increased upon laser irradiation (Fig. S9). After laser irradiation for 10 min without flowing saline solution, the temperature increased in the phantoms that contained SWNHox-BSA or ZnPc-SWNHox-BSA by ≈11–20°C, depending on the quantity of SWNHox (solid lines). The phantom without SWNHox increased only 4°C after 10 min of irradiation without flowing saline.

With the addition of flowing saline solution, laser irradiation for 10 min increased the temperature in the phantoms that contained SWNHox-BSA or ZnPc-SWNHox-BSA by ≈6–10°C, depending on the quantity of SWNHox (broken lines). The increase in the control, which lacked SWNHox, was ≈2°C. These results reveal that the temperature increase due to laser irradiation was considerably higher in the presence of SWNHox even under flowing-saline condition.

*In vivo*, the actual blood flow rate in tumor tissue probably corresponds to a value somewhere between our saline flow and no-flow conditions (since the flow of saline mimics blood flow in normal tissue). The blood flow rate in tumors generally decreases as the tumor size increases due to the progressive deterioration of vascular beds and to the rapid growth of the tumor cell population relative to the vascular beds. Therefore, the temperature increase caused by SWNHox PHT in normal tissues may be countered by the cooling effect of blood flow, but the temperature increase in tumor tissues may not be countered as quickly because of reduced blood flow. Thus, the increase in temperature caused by 10-min laser irradiation of the SWNHox-containing phantoms (Fig. S9) suggests that the 15-min laser irradiation of tumors in mice also increased the temperature of the subcutaneously transplanted tumors in which SWNHox-BSA or ZnPc-SWNHox-BSA was injected intratumorally before irradiation.

1 Tanaka H, *et al.* (1981) Physical basis of RF hyperthermia for cancer therapy: (2) Measurement of distribution of adsorbed power from radiofrequency exposure in agar phantom. *J Radiat Res* 22:101–108.

2 Hiroe A, Saito K, Takahashi M, Ito K (2007) Development on phantom for measurement of temperature rises inside biological tissue by electromagnetic waves exposure. *IEICE Trans Commun* J90-B:1187–1192.

3 Terada N, Amemiya Y (1984) The performance of the dipole array applicator for radiofrequency hyperthermia. *IEICE Trans Commun* J67-B:163–170.

4 Van Den Berg P, De Hoop A, Segal A, Praagman N (1983) A computational model of the electromagnetic heating of biological tissue with application to hyperthermic cancer therapy. *IEEE Trans Biomed Eng* 12:797–805.

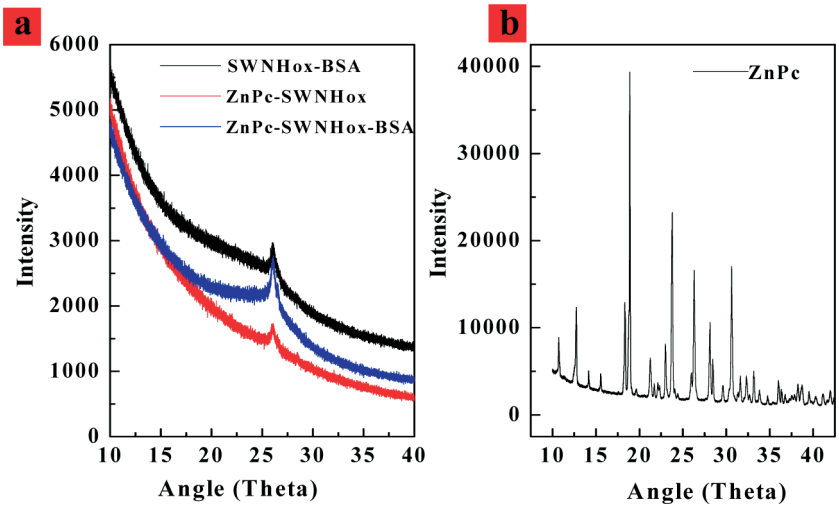


**Fig. S1.** X-ray diffraction analysis of SWNHox-BSA (*a*, black line), ZnPc-SWNHox (*a*, red line), ZnPc-SWNHox-BSA (*a*, blue line), and ZnPc (*b*, black line).

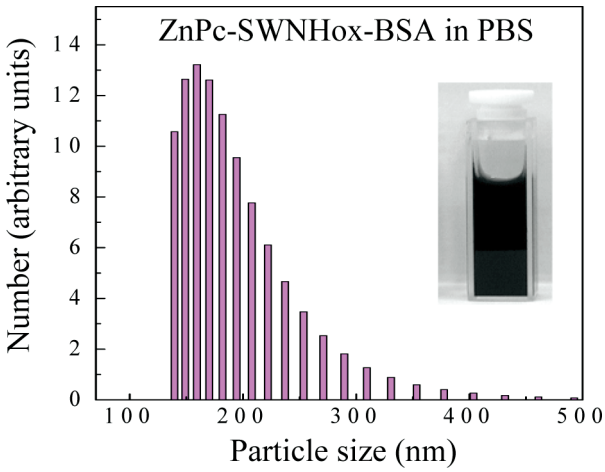


**Fig. S2.** Particle size of ZnPc-SWNHox-BSA dispersed in PBS. (*Inset*) Homogeneous dispersion of ZnPc-SWNHox-BSA.

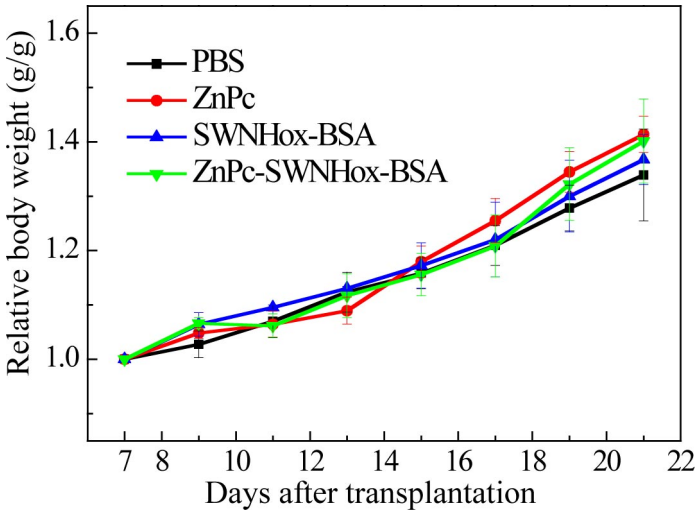


**Fig. S3.** Relative body weight of mice in the PDT-PHT testing period.

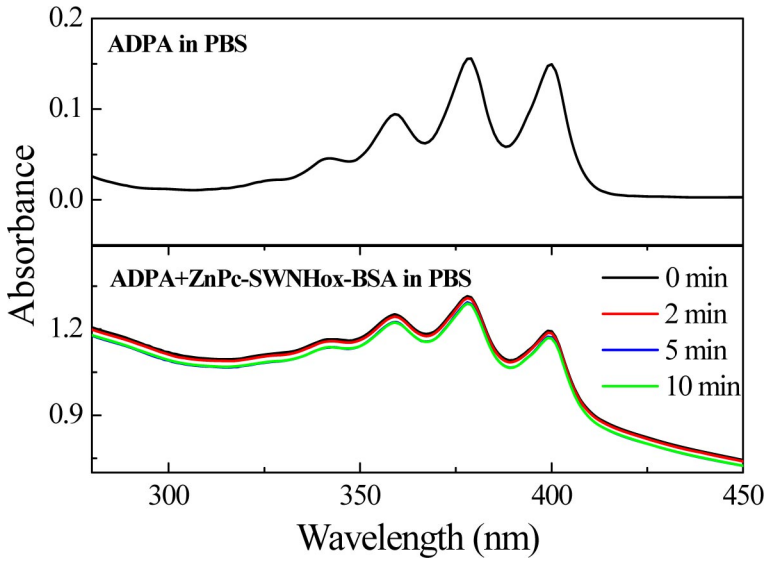


**Fig. S4.** (*a*) Absorption spectra of ADPA dissolved in PBS, and ADPA after mixed with ZnPc-SWNHox-BSA and light irradiation (650–750 nm, 0–10 min). (*b*) Optical absorption spectra of an aqueous dispersion of ZnPc-SWNHox-BSA and an ethanol solution of ZnPc. (*c*) Steady-state absorption spectra of ZnPc-SWNHox-BSA measured in a Ar-saturated aqueous solution after five exposures to 532-nm YAG laser light (≈3 mJ per pulse, 6-ns pulse width) in the presence of 1.0 mM $MV^{2+}$ and 1-benzyl-1,4-dihydronicotinamide (BNAH): (*i*) 0, (*ii*) 0.5, (*iii*) 1.0, (*iv*) 2.0, and (*v*) 3.0 mM BNAH.

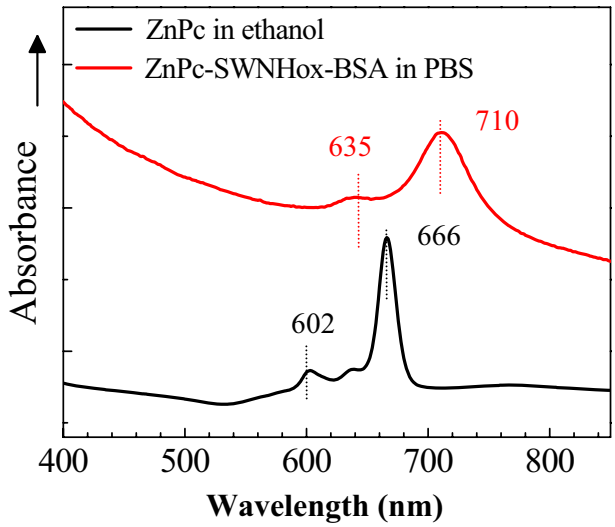
ZnPc in ethanol
ZnPc-SWNHox-BSA in PBS
Absorbance
635
710
666
602
400
500
600
700
800
Wavelength (nm)

Figure S4b

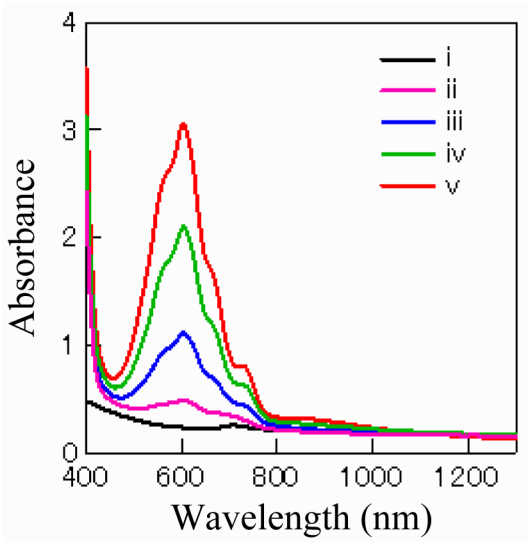
Absorbance
Wavelength (nm)
i
ii
iii
iv
v
0
1
2
3
4
400
600
800
1000
1200

**Figure S4c**

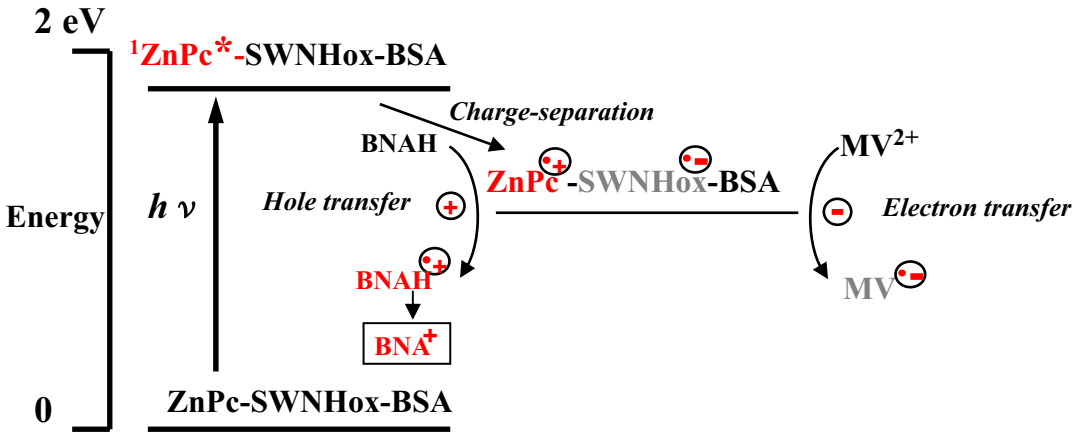


**Fig. S5.** Possible photoinduced processes of ZnPc-SWNHox-BSA in the presence of $MV^{2+}$ and BNAH in an Ar-saturated aqueous solution after exposure to 532-nm YAG laser light. $BNA^+$: 1-benzylnicodineamide cation.

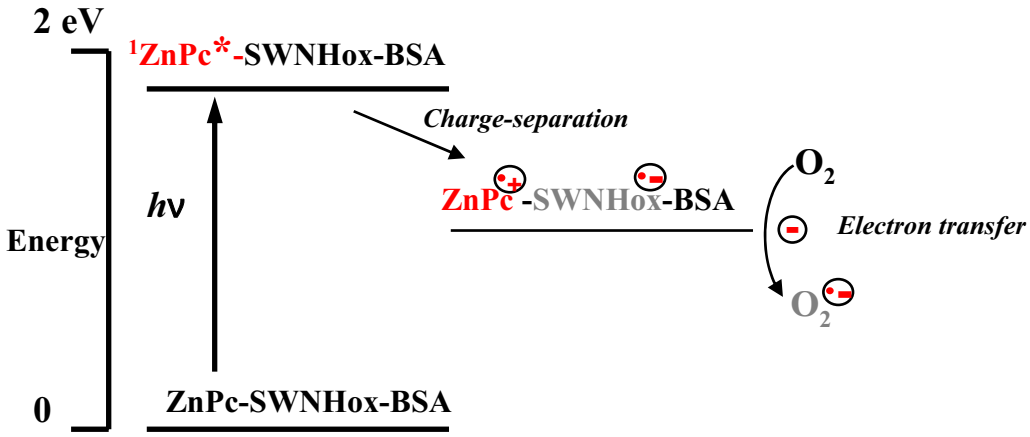


**Fig. S6.** Possible photoinduced processes of ZnPc-SWNHox-BSA in the presence of $O_2$. During *in vivo* and *in vitro* experiments under aerobic conditions, $O_2$ accepts an electron from the charge separated state, generating $O_2^{\bullet-}$.

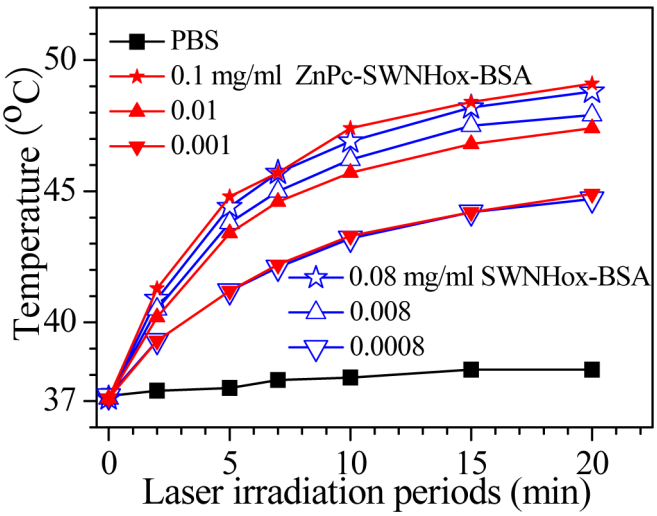


**Fig. S7.** Temperature increases of PBS and PBS dispersions of ZnPc-SWNHox-BSA and SWNHox-BSA upon irradiation with a 670-nm laser.

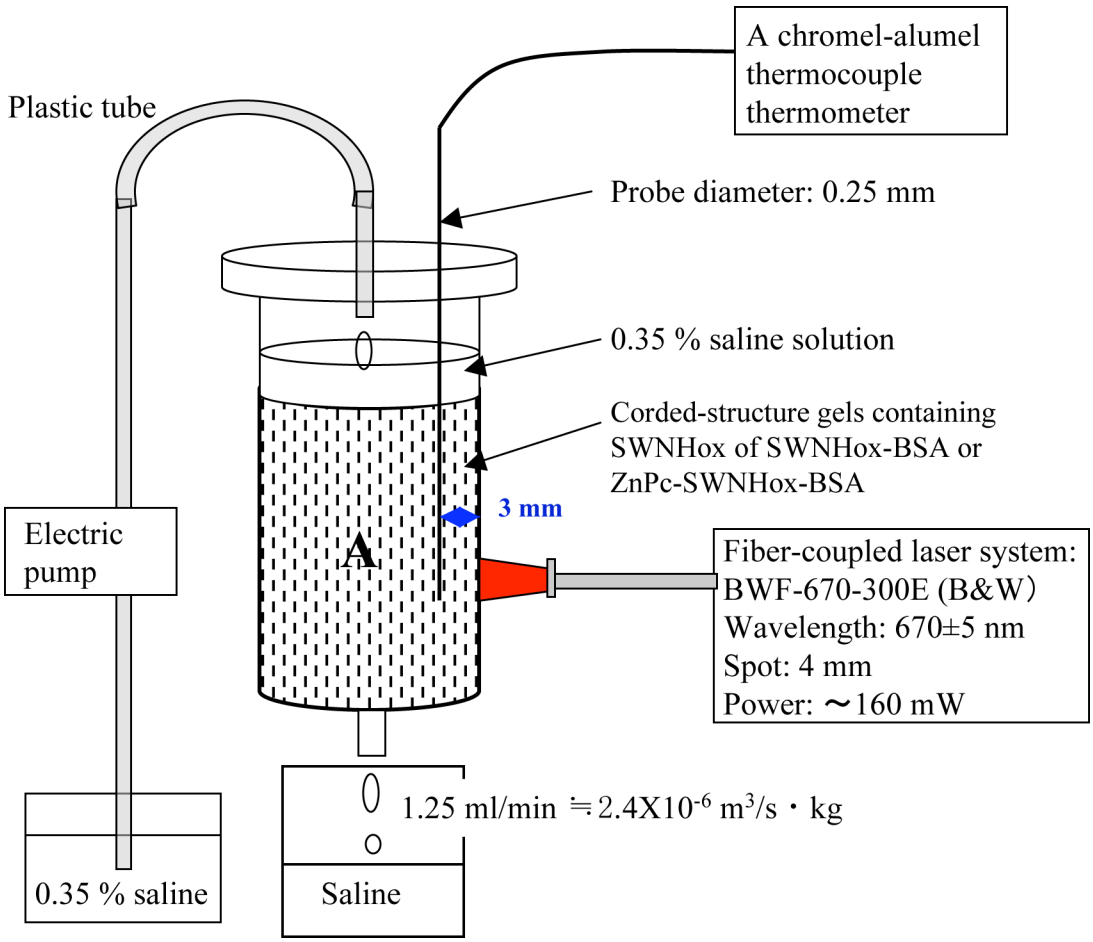


**Fig. S8.** Phantom experiment set-up. A 10-ml syringe was filled with corded structure agar gels (2% agar and 0.5% NaCl by weight). The agar also contained SWNHox-BSA or ZnPc-SWNHox-BSA (SWNHox: 0, 0.01, or 0.001% by weight).

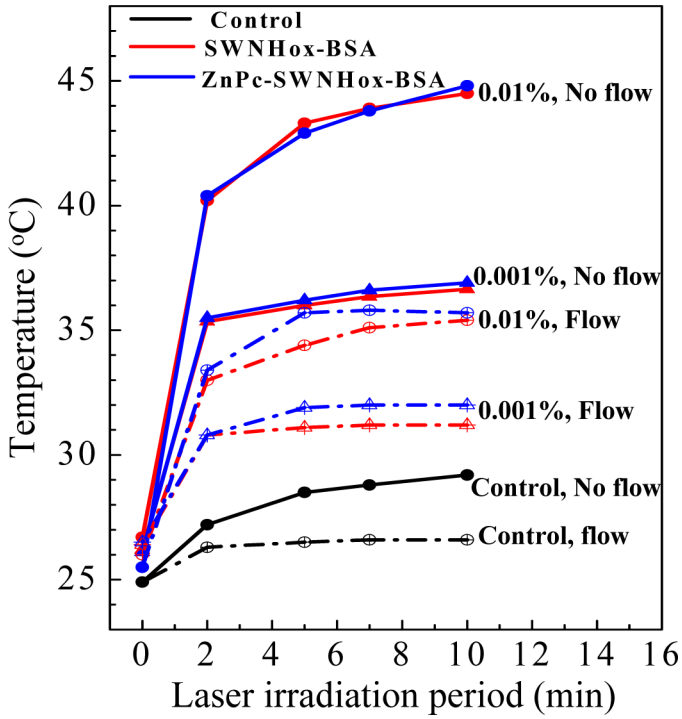


**Fig. S9.** The temperature increased in phantoms upon irradiation with a 670-nm laser for 0–10 min with (solid lines) and without (broken lines) flowing saline solution (1.25 ml/min). The red and blue lines indicate that SWNHox-BSA and ZnPc-SWNHox-BSA were added at the indicated concentrations of SWNHox. The black lines show the temperature changes of phantoms without additive SWNHox or ZnPc-SWNHox-BSA (control).